Advances in Science and Technology Research Journal

Advances in Science and Technology Research Journal, 2026, 20(3), 87–97
https://doi.org/10.12913/22998624/213647
ISSN 2299-8624, License CC-BY 4.0

Received: 2025.09.18
Accepted: 2025.11.27
Published: 2026.02.01

Effect of ground control point spacing on unmanned aerial vehicle orthomosaic and elevation model accuracy

Piotr Bożek[1], Arkadiusz Doroż[1*], Jarosław Taszakowski[1], Jarosław Janus[1]

1 Faculty of Environmental Engineering and Geodesy, University of Agriculture in Krakow, al. Mickiewicza 21, 31-120, Kraków, Poland
* Corresponding author's e-mail: arkadiusz.doroz@urk.edu.pl

ABSTRACT

The aim of this study was to analyze how the distance between ground control points (GCPs) affects the accuracy of orthophotomaps and elevation data generated from unmanned aerial vehicle (UAV) imagery. Unlike most previous research focused on small areas or GCP density per unit area, this study examines a large area of 3027 ha and introduces a spacing-based approach to define GCP distribution. A total of 48,000 images and 216 GCPs were used, with seven data processing variants differing in minimum GCP spacing (0–2500 m) and control-check point configurations. The results show that increasing GCP spacing does not significantly affect horizontal accuracy (X, Y) but significantly reduces elevation accuracy (Z) and overall spatial accuracy (XYZ). Moreover, once a spacing threshold of about 1000 m is exceeded, further increases have little effect on data quality. The findings highlight the possibility of optimizing the number and placement of GCPs without substantial loss of accuracy, which can greatly reduce the cost and duration of UAV mapping over large areas.

Keywords: UAV photogrammetry, GCP, orthophotomap, XYZ accuracy, elevation model, DTM, DSM.

INTRODUCTION

Photogrammetry is one of the key technologies used for acquiring precise spatial data. Its development in recent decades has significantly influenced the improvement of mapping accuracy and 3D surface reconstruction (Kovanič, 2023, Remondino et al., 2012), which is of great importance in such fields as land surveying (El Meouche et al., 2016), civil engineering (Tkáč and Mésároš, 2019), or archaeology (Marín-Buzón et al. 2021). The use of this technology allows for the generation of orthophotomaps, digital terrain models (DTM), and digital surface models (DSM), which are essential in spatial analyses and decision-making processes (Geng et al., 2018).

Traditional photogrammetric studies were carried out using aerial photographs taken from manned aircraft. Although effective, these methods were costly and required complex logistics, which limited their availability in many applications. However, with the development of unmanned aerial vehicle (UAV) technology, new opportunities have emerged in the field of photogrammetric data acquisition. UAVs offer not only greater operational flexibility and the possibility of carrying out missions in difficult-to-access areas, but also lower implementation costs and the ability to acquire images with very high spatial resolution (Remondino et al., 2012). The use of UAVs in photogrammetry significantly reduces the influence of atmospheric conditions and allows for the rapid execution of photogrammetric missions, even over small areas (Fras et al., 2020). This makes the technology increasingly widespread.

However, the quality of the images alone is not sufficient – equally important as resolution is the accuracy of the final product, understood as achieving the smallest possible positional errors of photographed terrain features. From this point of view, a key aspect in the process of generating an orthophotomap or 3D model is the correct configuration of the set of ground control points (GCP) (Ai et al., 2015, Zietara, 2017). Such points

are used in the process of image orientation and georeferencing of 3D models and orthophotomaps (Grayson et al., 2018). They are an essential element of every precise terrain reconstruction, enabling correct representation of the real geometry of the photographed area (Martínez-Carricondo et al., 2018). Proper configuration of the set of GCPs allows for the reduction of geometric errors resulting from optical imperfections, irregular terrain topography, and non-uniform lighting conditions during UAV flights (Ai et al., 2015, Yang et al., 2022). The use of GCPs ensures high accuracy of object positioning in the image relative to the real coordinate system. They also allow for correct alignment of the photo mosaic and elimination of external orientation errors, which may lead to deformations of the orthophotomap. It should be mentioned that photogrammetric studies may also be carried out without the use of GCPs, either to optimize costs or due to the characteristics of the study area, e.g. its difficult accessibility (Liu et al., 2021).

GCPs can be natural or artificial. Natural control points are characteristic landscape features such as road intersections, building corners, curbs, shorelines, or other distinct elements of existing infrastructure, which are easy to identify in aerial and UAV images (Rabins et al., 2023). Their advantage is the lack of necessity for additional marking in the field, but they may be less accurate, especially if their position is not clearly defined. Artificial control points are specially prepared markers placed in the field before carrying out a UAV mission. They are clearly visible in the images and have precisely determined geodetic coordinates, which makes them more reliable in the context of precise georeferencing.

One of the important issues in UAV photogrammetry is determining the optimal number and distribution of GCPs, which will ensure the highest accuracy of the orthophotomap or digital terrain model (Seo et al., 2024). For this reason, this problem has been the subject of many studies (Zhang et al., 2022; Ferrer-González et al., 2020, Gindraux et al., 2017; Sanz-Ablanedo et al., 2018, Yu et al., 2020, James et al., 2017, Liu et al., 2022, Shu et al., 2023, Villanueva et al., 2019). Too few control points may result in inaccurate image registration, deformations in the orthomosaic, and errors in terrain model reconstruction. This may lead to georeferencing shifts, incorrect elevation representation, and inconsistencies with real-world terrain coordinates. On the other hand, excessive density of GCPs, although it improves model accuracy, increases the time consumption and operational costs of the entire process (Ferrer-González et al., 2020; Zhao et al., 2024). Each additional point requires precise geodetic measurement, which involves the use of high-accuracy GNSS receivers and additional work. In the case of large areas, an excessive number of GCPs may significantly extend UAV survey preparation time.

Typical problems resulting from improper GCP configuration include edge deformations caused by the absence of control points near the boundaries of the surveyed area, leading to misaligned images. Another common issue is georeferencing shifts, which create inconsistencies between the orthophotomap and the real coordinate system and can have serious implications in precise surveying applications. Improper GCP placement may also cause disturbances in elevation reconstruction, resulting in inaccurate terrain relief representation, particularly in areas with significant topographic variation. To achieve optimal results, it is necessary to find a compromise between the resulting mapping accuracy and operational efficiency. In practice, the number of GCPs should be adjusted to two most important aspects. The first is terrain characteristics – in flat areas it is possible to use a sparser configuration of GCPs, while in mountainous and urbanized areas higher density is required. The second is accuracy requirements – in surveying applications, centimeter-level precision requires a dense set of GCPs, whereas in environmental and agricultural analyses lower density may be acceptable.

Proper planning of the number and distribution is therefore crucial for obtaining high-quality photogrammetric products. Planning includes not only determining the appropriate number and placement of points, but also their geodetic measurements using precise GNSS receivers. Combined with appropriate data processing methods, a well-planned GCP configuration allows for obtaining highly accurate and reliable results in the process of creating an orthophotomap and 3D terrain models.

Research results clearly indicate that the use of GCPs improves the accuracy of UAV survey results both in terms of the resulting orthophotomap and elevation models (Agüera-Vega et al., 2017). However, the time- and cost-intensity of this stage of work, related to the distribution and measurement of the set of GCPs, poses major challenges (Dharshan Shylesh et al., 2023) and may be significantly higher than the stage of acquiring and

processing aerial images itself. For this reason, research on the optimization of the number of GCPs is valuable, as significant research gaps can still be identified among existing results. One of the observed gaps is the lack of studies on GCP density, understood as finding the relationship between the distance between individual GCPs and the accuracy of the obtained results. Importantly, the vast majority of existing studies have been carried out for areas of small size.

The aim of this study is to analyze how GCP distribution density, particularly the minimum distance between points, affects the accuracy of UAV-derived orthomosaics and elevation data. The analysis was conducted over a large area of 3,027 ha and included several GCP spacing scenarios. The results provide valuable insights for optimizing photogrammetric processes in engineering, surveying, and environmental applications. It is expected that the findings will help identify the optimal number of control points required to maintain high mapping accuracy while improving operational efficiency and reveal a threshold beyond which additional GCPs no longer enhance accuracy but only increase time and cost.

STUDY AREA

The study area covered eight localities located in the Charsznica commune: Szarkówka, Podlesice, Uniejów-Kolonia, Swojczany, Charsznica, Witowice, Dąbrowiec, and Ciszowice. The total surface area of the analyzed region was 3,027.38 ha. This area is situated in Miechów County, Lesser Poland Voivodeship, in southern Poland. The land is predominantly agricultural, characterized by individual farms and a highly fragmented ownership structure. The choice of location was directly related to preparatory work for a land consolidation project, where precise spatial data are essential for designing new parcel boundaries and improving land management efficiency.

Although the analyses had a planning background, the key factor in selecting this area for research was its complex morphology. The terrain features significant elevation differences, numerous ravines, valleys, and hills, which pose major challenges in generating accurate digital orthomosaics from UAV data, particularly regarding the influence of GCP distribution on product accuracy.

The main objective of the study was to assess the precision of the digital orthomosaic as a function of the number and distribution of GCPs. Due to its diverse relief and height variations, the area provided an ideal testing ground for evaluating how GCP configuration affects the accuracy of UAV-derived photogrammetric products (Figure 1).

METHODOLOGY

The objective of the presented methodology was to examine the impact of GCP density on the accuracy of models created using unmanned aerial vehicles. In order to investigate the influence of GCP density on the accuracy of the resulting

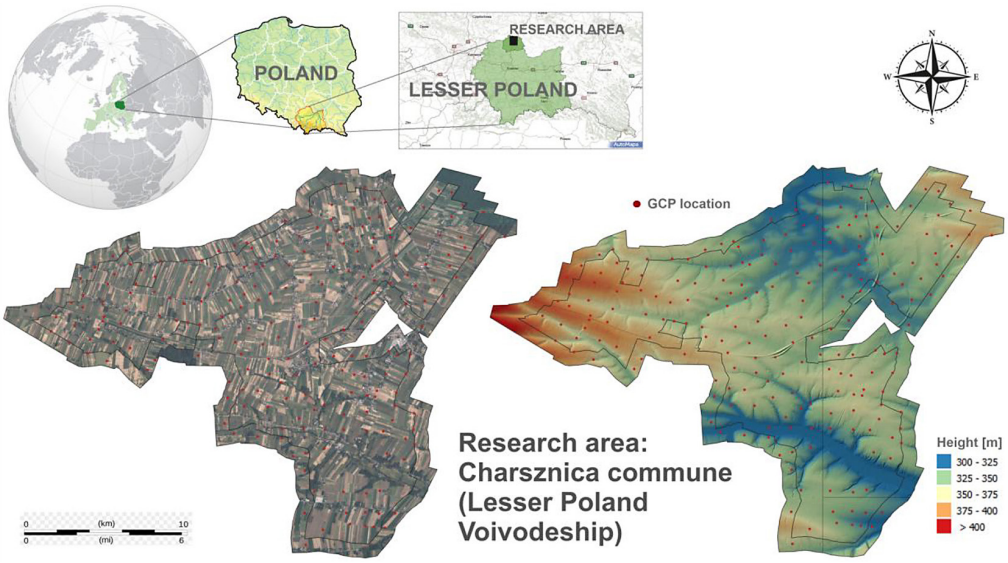

Figure 1. Location of the study area on the background of the orthophotomap and the digital terrain model

orthomosaic, it was first necessary to define the method of identifying this density. One alternative is to determine the number of control points per unit of area. Another possible approach is to define the minimum distance between control points. The second option was chosen, particularly since this type of approach (analysis of different spacing values between GCPs) has not yet been addressed in any of the existing studies.

The methodology consisted of three stages: data acquisition, processing, and analysis. The first stage involved data acquisition using a WingtraOne GEN II VTOL UAV, equipped with a Sony RX1R II camera, capturing vertical (nadir) images. A total of 48,000 photographs were collected, covering an area of 26.185 km², with missions planned so that the ground sampling distance ranged from 0.02 to 0.03 m, and with 65% side and forward overlap. Flights were conducted at an altitude of 100–120 m. Within the study area, 216 GCPs were established. The points were marked using target plates with white crosses placed on hardened surfaces. At each GCP, geodetic measurements were carried out using the RTK technique with a Trimble R2 GNSS receiver, achieving an accuracy of 0.03 m for horizontal coordinates and 0.06 m for elevation. The UAV recorded GNSS corrections, saving the coordinates of image projection centers for the acquired photographs. The data were collected over the course of 32 missions (Figure 2).

The second stage involved data processing in Agisoft Metashape software. In the first step, all images were imported into a single "Chunk," and then accuracy parameters were defined for the acquired data: camera accuracy was set to 0.1 m for horizontal coordinates and 0.2 m for vertical coordinates, and the accuracies for markers corresponded to the values obtained from the Trimble R2 GNSS receiver. In the "Image Coordinates Accuracy" settings, marker accuracy was set to 1 pixel, while tie point accuracy was set to 2 pixels. In the "Reference Settings" section, the "capture distance" parameter was set to 120 m, corresponding to the typical flight altitude. Additionally, the project's coordinate system was defined in accordance with the PL-2000 system (EPSG:2178), transforming the projection center coordinates from the WGS 84 system (EPSG:4326) into PL-2000 using the Convert tool available in Agisoft Metashape.

The next step consisted of importing the GCP dataset and calculating the Quality parameter, which enabled the exclusion from processing of images with low quality (coefficient below 0.8). Then, the prepared "Chunk" was duplicated six times, each one characterized by a different configuration of parameters affecting the number of GCPs used. In the first case, all 216 available GCPs were included for adjustment (Variant "ALL"). In the second, assuming a distance between points not greater than 500 m (Variant "500"), 83 GCPs were selected. In the third, with a minimum spacing of 1000 m (Variant "1000"), 28 GCPs were obtained. Similarly, for a minimum spacing of 1500 m, the number of control points was 17 (Variant "1500"). In the next chunk, a minimum spacing of 2000 m was assumed, which resulted in the use of 10 GCPs (Variant "2000"). In the following step (Variant "2500"), only 7 control points were used. In the final variant ("OFF"), all 216 points were treated as checkpoints for which accuracy verification was carried out, while the number of GCPs was 0.

For the prepared Chunks, the photo alignment process (Align Photos) was performed, with Accuracy set to High, Key point limit to 10.000, and Tie point limit to 4.000. The Generic preselection option was also enabled. After photo alignment, camera parameters (f, k1, k2, k3, cx, cy, p1, p2) were optimized, excluding from the process those images with a Quality coefficient below 0.8. After optimization, the photo alignment process (Align Photos) was repeated, reintroducing the previously excluded images. The results obtained in this way (estimated coordinates for the used GCPs and the set of checkpoints) for each variant were exported to text files and analyzed.

To ensure comparability across all test variants, the same set of 216 points was used as checkpoints in each case. Although an alternative approach – using a variable number of checkpoints defined as n = 216 – number of GCPs used – was possible, it was not adopted for two main reasons.

First, this method would exclude the "ALL" configuration from comparative analysis, since in that case no checkpoints would remain. Second, it would lead to inconsistent sample sizes between variants, making direct comparison of accuracy metrics difficult. Therefore, using a constant set of 216 checkpoints provided uniform statistical conditions for evaluating differences among the tested GCP configurations.

RESULTS

For each of the seven GCP distribution variants, positional accuracies were calculated for

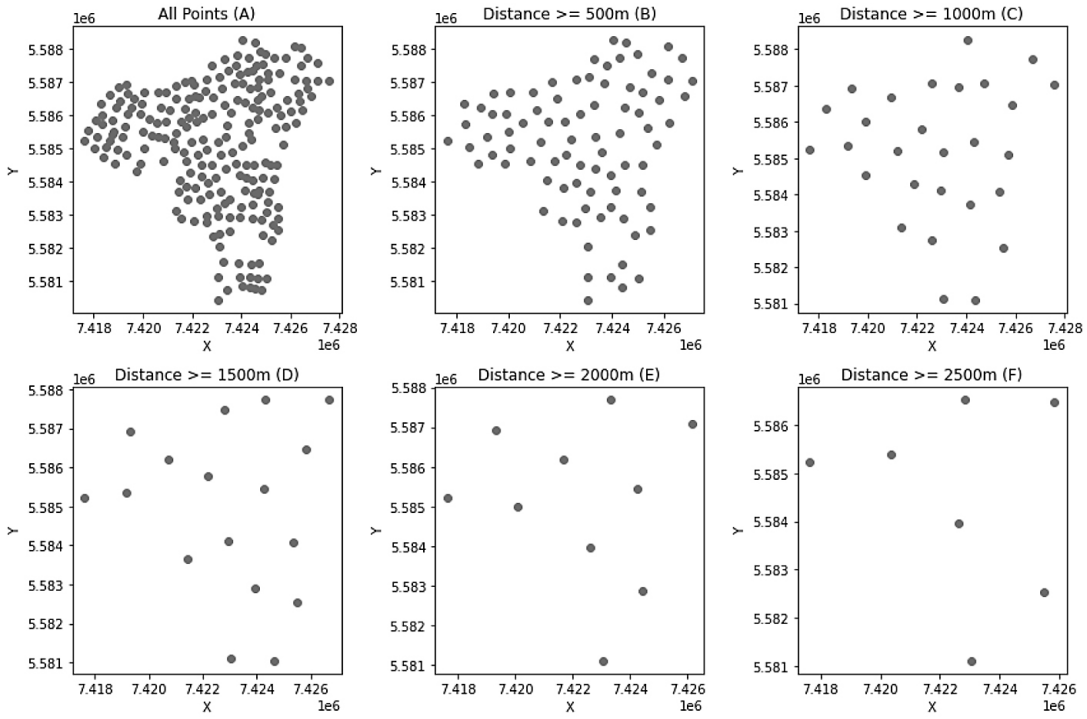

Figure 2. GCP configuration variations considered in the study

216 checkpoints in five categories: X, Y, Z, XY, and XYZ. The basic statistics of this dataset are presented in Tables 1 and 2.

The variability of the obtained accuracies for individual points in each category is clearly visible in the form of scatter plots. However, the high density of points, even when using an appropriate color scale, makes such plots difficult to read. For this reason, it was decided to visualize two categories most distant from each other in terms of obtained accuracies: ALL and OFF, that is, the variant in which all 216 points were used as GCPs compared to the variant in which the data were processed without the use of any GCPs. For the X, Y, Z, and XY categories, these plots are shown in Figure 3. The most important plot of this series, presenting the differences in point coordinate accuracy in the XYZ variant, is shown in Figure 4.

The final form of presenting the most important results of study is the linear relationship between the distance between GCPs (including also the two extreme configurations: ALL (XX m) and OFF (no GCPs)) and the average magnitude of a given type of error, presented in Figure 5.

To better assess the impact of changes in GCP distribution density on the obtained results, they were also presented as line charts after first ordering the points according to the obtained positional error values. Similarly to before, in the first visualization (Figure 6) the variability of the obtained errors of individual coordinates (X, Y, Z) and the positional error in the plane (XY) was presented.

The last category (positional error in three-dimensional space, XYZ) was presented in the form of two figures. The first one (analogous to Figure 3) takes the form of a line chart of data sorted according to the error value (Figure 6 and 7). The second shows histograms of XYZ error magnitudes for individual GCP configurations (densities) (Figure 8).

DISCUSSION

The obtained results constitute another significant contribution to the knowledge on the influence of GCP set parameters used in the processing of UAV-acquired imagery – in this case, the positional accuracy of points in several categories (X, Y, Z, XY, XYZ) was analyzed as a function of GCP density defined by the minimum distance between individual GCPs.

Three of the most important observed relationships can be identified. The first is the practical lack of observed influence of the number of GCPs on planar coordinate errors (X, Y, and XY) (Figure 8). The reason in this case may be the favorable weather conditions during the flight combined with high-quality GNSS signals and good-quality receivers. The second observation is the significant

Table 1. Basic characteristics of positional errors of checkpoints for individual error categories and GCP configurations (horizontal errors)

GCP configuration name	Error category	Min [m]	Max [m]	Mean [m]	Median [m]	Std. dev. [m]
ALL	X_error	0.00	0.08	0.02	0.01	0.01
	Y_error	0.00	0.09	0.02	0.02	0.02
	XY_error	0.00	0.09	0.03	0.03	0.02
500	X_error	0.00	0.10	0.02	0.02	0.02
	Y_error	0.00	0.09	0.02	0.01	0.02
	XY_error	0.00	0.12	0.03	0.03	0.02
1000	X_error	0.00	0.10	0.02	0.02	0.02
	Y_error	0.00	0.09	0.02	0.02	0.02
	XY_error	0.00	0.11	0.03	0.03	0.02
1500	X_error	0.00	0.14	0.02	0.02	0.02
	Y_error	0.00	0.09	0.02	0.02	0.02
	XY_error	0.00	0.14	0.03	0.03	0.02
2000	X_error	0.00	0.14	0.02	0.02	0.02
	Y_error	0.00	0.09	0.02	0.02	0.02
	XY_error	0.00	0.14	0.03	0.03	0.02
2500	X_error	0.00	0.14	0.02	0.02	0.02
	Y_error	0.00	0.09	0.02	0.02	0.02
	XY_error	0.00	0.14	0.03	0.03	0.02
OFF	X_error	0.00	0.14	0.02	0.02	0.02
	Y_error	0.00	0.09	0.02	0.02	0.02
	XY_error	0.00	0.14	0.03	0.03	0.02

Table 2. Basic characteristics of positional errors of checkpoints for individual error categories and GCP configurations (vertical errors)

GCP configuration name	Error category	Min [m]	Max [m]	Mean [m]	Median [m]	Std. dev. [m]
ALL	Z_error	0.00	0.21	0.10	0.10	0.05
	XYZ_error	0.01	0.21	0.10	0.11	0.05
500	Z_error	0.00	0.24	0.12	0.14	0.06
	XYZ_error	0.01	0.24	0.13	0.14	0.06
1000	Z_error	0.00	0.27	0.14	0.16	0.07
	XYZ_error	0.01	0.27	0.15	0.17	0.07
1500	Z_error	0.00	0.28	0.15	0.17	0.07
	XYZ_error	0.01	0.28	0.15	0.18	0.07
2000	Z_error	0.00	0.28	0.15	0.17	0.07
	XYZ_error	0.01	0.28	0.16	0.18	0.07
2500	Z_error	0.00	0.28	0.15	0.18	0.07
	XYZ_error	0.01	0.28	0.16	0.18	0.07
OFF	Z_error	0.00	0.28	0.15	0.18	0.07
	XYZ_error	0.01	0.29	0.16	0.19	0.07

influence of the number of GCPs on the accuracy of the Z coordinate of the determined points (and consequently also on the total positional error of the point in three-dimensional space, XYZ). The cause can be attributed to the large elevation differences in the analyzed area, exceeding 100 meters (Figure 1 or as part of the first figure). This at the same time indicates the absolute necessity of using GCPs in areas with highly diverse terrain relief.

The third important observation is the nonlinear relationship between changes in the distance between GCPs and changes in the average magnitude of errors in a given category (Figure 8). In practice (as can be clearly seen in Figure 8, XYZ error), significant differences in accuracy are visible between the ALL and 500 modes, as well as between the 500 and 1000 modes. Further increasing the distance does not result in a significant

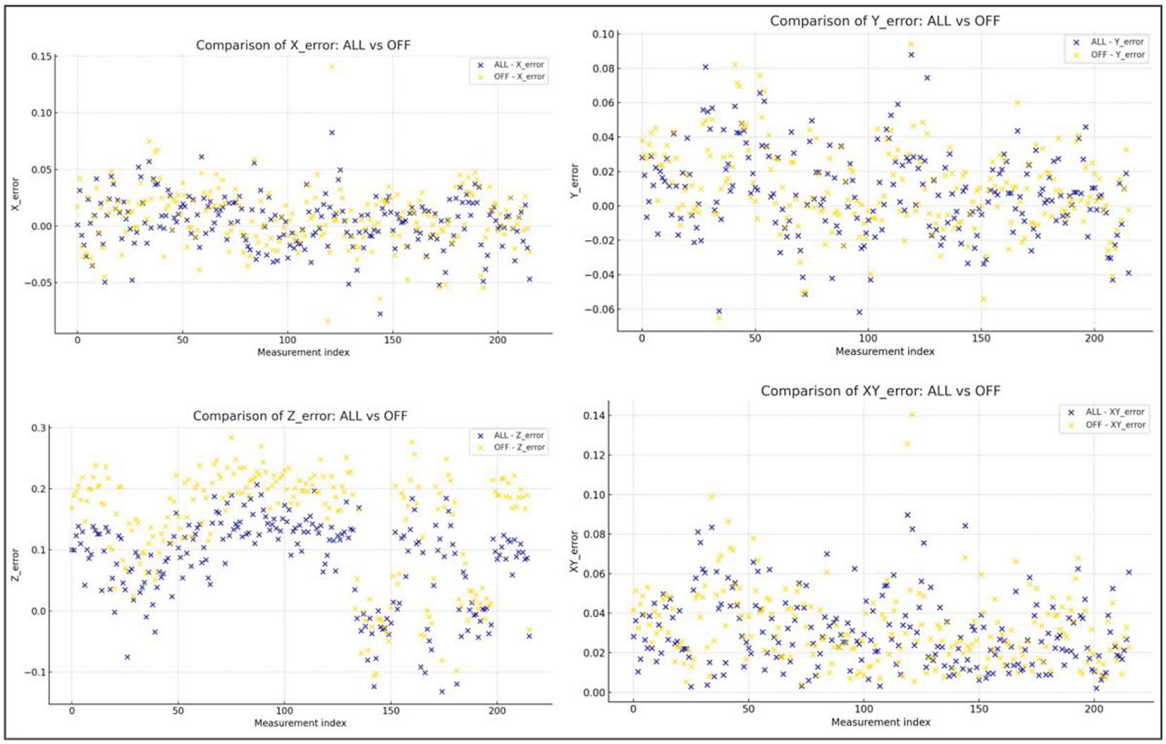

Figure 3. Variations in error magnitudes at checkpoints in the categories: X, Y, Z, and XY for two variants: ALL (all GCPs used), and OFF (no GCPs used)

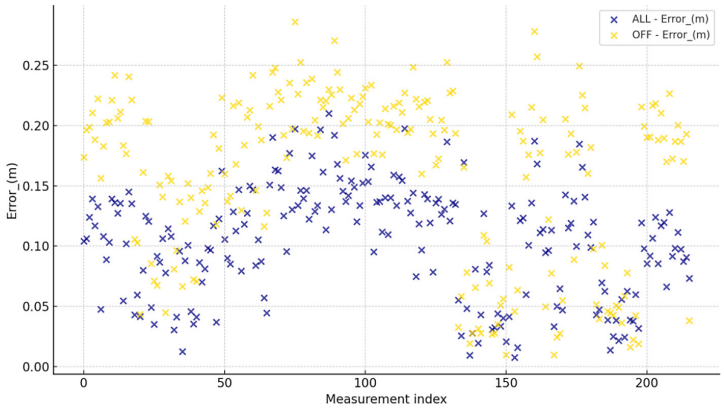

Figure 4. Variations in error magnitudes at checkpoints in the XYZ category for two variants: ALL (all GCPs used), and OFF (no GCPs used)

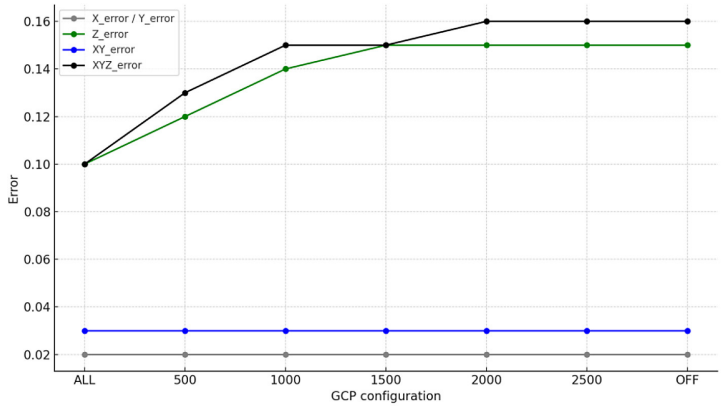

Figure 5. Relationship between the mean error values of a given category and GCP configuration (ALL – all GCPs used, OFF, no GCPs used)

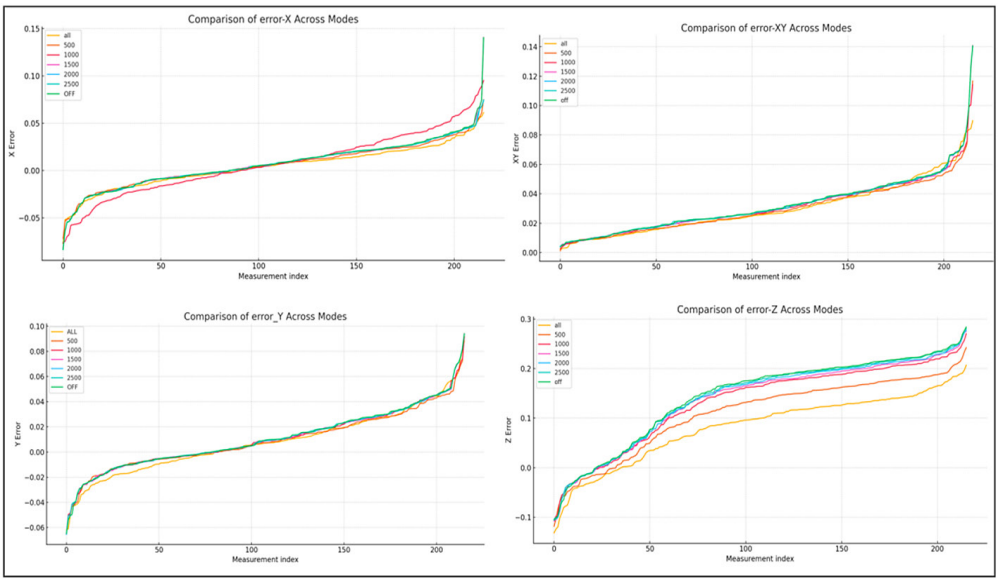

Figure 6. Error magnitudes at checkpoints – line chart with data sorted by error values (ALL: all GCPs used, OFF: no GCPs used)

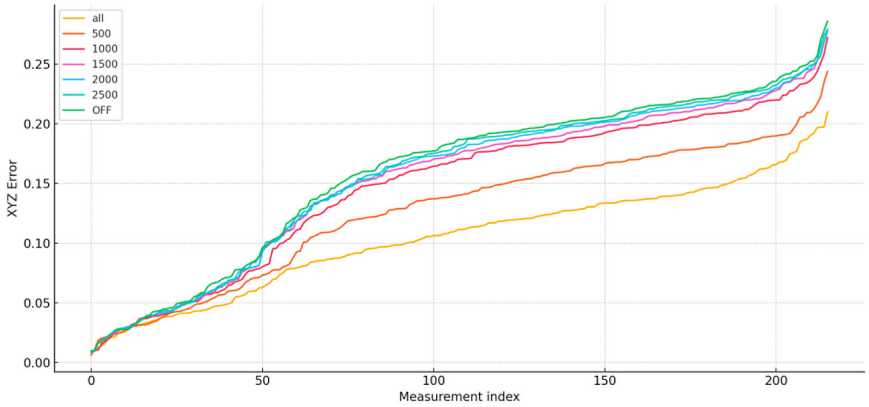

Figure 7. Error magnitudes at checkpoints in the XYZ category – line chart with data sorted by error values (ALL: all GCPs used, OFF: no GCPs used)

deterioration of accuracy (though this note still applies to the accuracy of the Z and XYZ parameters). It is definitely worthwhile to use a dense network of GCPs in all cases where high accuracy of elevation data is required and at the same time the area features large elevation differences.

Reference should be made here to other studies that have attempted to determine the relationships associated with the influence of GCP configuration on the accuracy of the resulting orthophotomap or elevation data. In studies conducted over a small area of the Pennsylvania State University campus (Bolkas, 2019), the optimal separation distance between GCPs was determined to be 105 m in order to obtain elevation accuracy at the level of 1–2 cm. In studies on the influence of GCP configuration over glaciated areas (Gindraux et al., 2017), the optimal GCP density was determined to be about 10 GCPs per km², above which the accuracy of the results no longer increased.

The analyzed OFF variant, meaning data processing without the use of GCPs, shows that such products can be created with accuracy acceptable (depending on the purpose of the product) even without the use of GCPs (Liu et al., 2021; Szypuła, 2024, Türk et al., 2022; Hugenholtz et al., 2016). The observations of this study are consistent with the results of other authors (Liu et al., 2022; Mallinis et al., 2017) and indicate the possibility of using this mode in areas with limited accessibility or when the budget for GCP coordinate surveying in the field is restricted. However, in such a case, the quality of the GNSS receivers on UAV systems plays an important role, and in

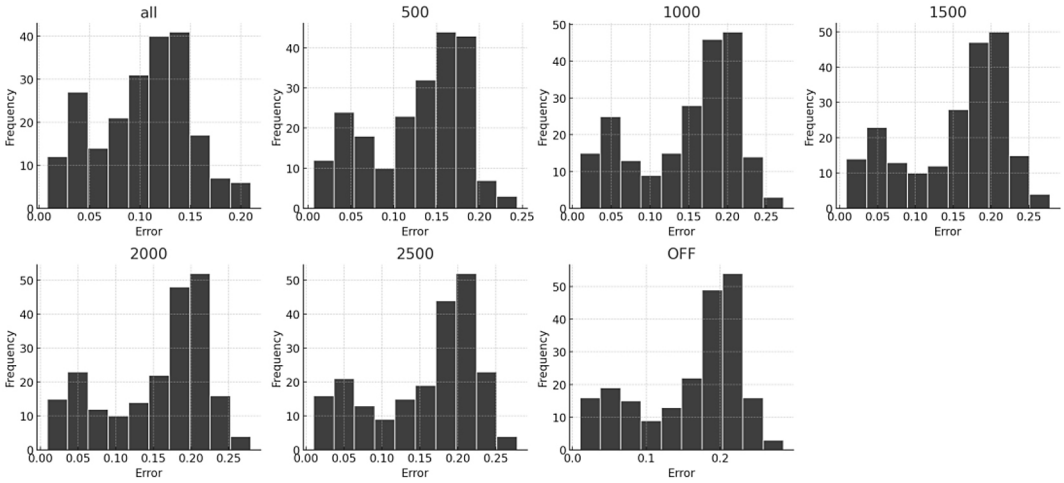

Figure 8. Histograms of checkpoint error sets in individual categories and for specific GCP configurations (ALL: all GCPs used, OFF: no GCPs used)

the case of low-quality receivers, including GCPs can improve the accuracy of the 3D model from a level of two meters to just a few centimeters.

Previous studies have emphasized the importance of adequate GCP density for minimizing elevation errors, though recommended values vary depending on the study scale and methodology. For smaller areas, a relatively high GCP density is advised (e.g., about 1 GCP per 200 m²; Oniga et al., 2018), while research on larger sites suggests that fewer, well-distributed points are sufficient to maintain accuracy. For instance, Martínez-Carricondo et al. (2018) recommend a general density of 0.5–1 GCP × ha^{-1}, and Yu et al. (2020) found that 12 to 18 GCPs were adequate for areas ranging from 7 to 342 ha.

The obtained results may be applied wherever a compromise must be considered between the accuracy of results and the effort required to prepare (distribute and measure) an appropriate number of GCPs for projects covering relatively large areas for UAV surveying. In the case analyzed in this manuscript, this involved the preparation of an orthophotomap and DEM data for land consolidation projects, but in practice these may be any products covering areas of several hundred or several thousand hectares. In such cases, the considered distances between GCPs (in multiples of 500 m) are worth considering in order to eliminate excessive numbers of GCP coordinate measurements as well as the process of setting them up in the field. For an area of 1000 ha, the densities recommended in other studies, at the level of 1 to 5 points/ha, would mean as many as 5000 GCPs, which seems economically unjustified. In such cases, an approach based on average distances between individual GCPs in the range of 500–2000 m (which of course can be converted into average GCP density per unit area) may represent a good compromise between the cost of the product and its accuracy.

It is also worth mentioning the weaknesses of this study, but at the same time the opportunities for further research in this field. The data were acquired at only one flight altitude and with one software package, which does not allow for evaluation of the influence of these factors on the accuracy of the output data, as was done, for example, in two studies (Oniga et al., 2018; Bolkas, 2019), although in those cases the study area was relatively small. Another weakness (though at the same time also an advantage) is the execution of the flight at a constant altitude relative to the take-off point, despite relatively large elevation differences in the study area. It would be valuable to compare the obtained results with those derived from maintaining a constant altitude relative to the terrain during the entire flight. These limitations of the study also point to opportunities for conducting more in-depth analyses in the future, which could provide answers to such research questions.

CONCLUSIONS

In this study, the relationship between GCP density and the accuracy of spatial data acquired from UAVs was analyzed. The focus was placed on the effect of the minimum distance between GCPs on the quality of the orthophotomap and the elevation model. The results clearly show that

GCP density has the greatest influence on the elevation coordinate (Z), and consequently on the overall spatial error (XYZ). For horizontal coordinates (X, Y), this influence was minor, indicating high stability of the reference system provided by high-quality GNSS sensors and favorable weather conditions.

A key practical finding is the identification of a saturation point, beyond which increasing GCP density yields no significant accuracy improvement. In this study, a spacing of approximately 1000 m between GCPs maintained acceptable elevation accuracy while substantially reducing the time and cost of fieldwork.

The analysis of the OFF variant (without GCPs) produced surprisingly good results, though with lower elevation accuracy. This suggests that, for applications such as environmental analyses, general inventories, or preliminary terrain assessments, the use of traditional GCPs may be optional if the UAV is equipped with a precise GNSS receiver. However, for tasks requiring high precision (e.g., land consolidation, infrastructure design, surveying), a well-planned GCP configuration remains essential.

The presented methodology is scalable and can be applied in both local and regional projects, where economic efficiency and data quality are equally important. Future research should explicitly explore different UAV platforms, various terrain types, and the potential integration of direct georeferencing methods to further refine the relationship between GCP density and data accuracy.

REFERENCES

1. Agüera-Vega, F., Carvajal-Ramírez, F., Martínez-Carricondo, P. Assessment of photogrammetric mapping accuracy based on variation ground control points number using unmanned aerial vehicle. Measurement: Journal of the International Measurement Confederation, 2017; 98. https://doi.org/10.1016/j.measurement.2016.12.002
2. Ai, M., Hu, Q., Li, J., Wang, M., Yuan, H., Wang, S. A robust photogrammetric processing method of low-altitude UAV images. Remote Sensing, 2015; 7(3). https://doi.org/10.3390/rs70302302
3. Bolkas, D. Assessment of GCP Number and Separation Distance for Small UAS Surveys with and without GNSS-PPK Positioning. Journal of Surveying Engineering, 2019; 145(3). https://doi.org/10.1061/(asce)su.1943-5428.0000283
4. Dharshan Shylesh, D. S., Manikandan, N., Sivasankar, S., Surendran, D., Jaganathan, R., Mohan, G. Influence of quantity, quality, horizontal and vertical distribution of ground control points on the positional accuracy of UAV survey. Applied Geomatics, 2023; 15(4). https://doi.org/10.1007/s12518-023-00531-w
5. El Meouche, R., Hijazi, I., Poncet, P. A., Abunemeh, M., Rezoug, M. UAV photogrammetry implementation to enhance land surveying, comparisons and possibilities. In International Archives of the Photogrammetry, Remote Sensing and Spatial Information Sciences - ISPRS Archives 2016; 42. https://doi.org/10.5194/isprs-archives-XLII-2-W2-107-2016
6. Ferrer-González, E., Agüera-Vega, F., Carvajal-Ramírez, F., Martínez-Carricondo, P. UAV photogrammetry accuracy assessment for corridor mapping based on the number and distribution of ground control points. Remote Sensing, 2020; 12(15). https://doi.org/10.3390/RS12152447
7. Fras, M. K., Drešček, U., Lisec, A., Grigillo, D. Analysis of the impacts on the quality of uav photogrammetric products. Geodetski Vestnik, 2020; 64(4). https://doi.org/10.15292/geodetski-vestnik.2020.04.489-507
8. Geng, J., Zhang, Y., Li, M., Geng, H., Wang, Y. Research on 3D dynamic visualization based on flood numerical simulation. Harbin Gongcheng Daxue Xuebao/Journal of Harbin Engineering University, 2018; 39(7). https://doi.org/10.11990/jheu.201704008
9. Gindraux, S., Boesch, R., Farinotti, D. Accuracy assessment of digital surface models from Unmanned Aerial Vehicles' imagery on glaciers. Remote Sensing, 2017; 9(2). https://doi.org/10.3390/rs9020186
10. Grayson, B., Penna, N. T., Mills, J. P., Grant, D. S. GPS precise point positioning for UAV photogrammetry. Photogrammetric Record, 2018; 33(164). https://doi.org/10.1111/phor.12259
11. James, M. R., Robson, S., d'Oleire-Oltmanns, S., Niethammer, U. Optimising UAV topographic surveys processed with structure-from-motion: Ground control quality, quantity and bundle adjustment. Geomorphology, 2017; 280. https://doi.org/10.1016/j.geomorph.2016.11.021
12. Kovanič, Ľ., Kovanic, L., Vlčko, J., Melicher, R. Review of Photogrammetric and LiDAR Applications of UAV. Applied Sciences, 2023; 13(11): 6732. https://doi.org/10.3390/app13116732
13. Liu, J., Xu, W., Guo, B., Zhou, G., Zhu, H. Accurate mapping method for UAV photogrammetry without ground control points in the map projection frame. IEEE Transactions on Geoscience and Remote Sensing, 2021; 59(11). https://doi.org/10.1109/TGRS.2021.3052466
14. Liu, W. C., Huang, W. C., Young, C. C. Uncertainty analysis for image-based streamflow measurement: The influence of ground control points. Water

(Switzerland), 2023; 15(1). https://doi.org/10.3390/w15010123

15. Liu, X., Lian, X., Yang, W., Wang, F., Han, Y., Zhang, Y. Accuracy assessment of a UAV direct georeferencing method and impact of the configuration of ground control points. Drones, 2022; 6(2). https://doi.org/10.3390/drones6020030
16. Mallinis, G., Patias, P., Giagkas, F., Georgiadis, C., Kaimaris, D., Tsioukas, V. Evaluating horizontal positional accuracy of low-cost UAV orthomosaics over forest terrain using ground control points extracted from different sources. Proc. SPIE 10444, Fifth International Conference on Remote Sensing and Geoinformation of the Environment (RSCy2017), 104440U (6 September 2017); https://doi.org/10.1117/12.2278008
17. Martínez-Carricondo, P., Agüera-Vega, F., Carvajal-Ramírez, F., Mesas-Carrascosa, F. J., García-Ferrer, A., Pérez-Porras, F. J. Assessment of UAV-photogrammetric mapping accuracy based on variation of ground control points. International Journal of Applied Earth Observation and Geoinformation, 2018; 72. https://doi.org/10.1016/j.jag.2018.05.015
18. Marín-Buzón, C., Pérez-Romero, A., López-Castro, J. L., Jerbania, I. Ben, Manzano-Agugliaro, F. Photogrammetry as a new scientific tool in archaeology: Worldwide research trends. Sustainability (Switzerland), 2021; 13(9). https://doi.org/10.3390/su13095319
19. Oniga, V.-E., Breaban, A.-I., Statescu, F. Determining the optimum number of ground control points for obtaining high precision results based on UAS images. Proceedings. 2018. https://doi.org/10.3390/ecrs-2-05165
20. Rabins, L. F., Theuerkauf, E. J., Bunting, E. L. Using existing infrastructure as ground control points to support citizen science coastal UAS monitoring programs. Frontiers in Environmental Science, 2023; 11. https://doi.org/10.3389/fenvs.2023.1101458
21. Remondino, F., Barazzetti, L., Nex, F., Scaioni, M., Sarazzi, D. Uav photogrammetry for mapping and 3d modeling – current status and future perspectives. The International Archives of the Photogrammetry, Remote Sensing and Spatial Information Sciences, 2012; XXXVIII-1/C22. https://doi.org/10.5194/isprsarchives-xxxviii-1-c22-25-2011
22. Sanz-Ablanedo, E., Chandler, J. H., Rodríguez-Pérez, J. R., Ordóñez, C. Accuracy of Unmanned Aerial Vehicle (UAV) and SfM photogrammetry survey as a function of the number and location of ground control points used. Remote Sensing, 2018; 10(10). https://doi.org/10.3390/rs10101606
23. Shu, S., Yu, O. Y., Schoonover, C., Liu, H., Yang, B. Unmanned aerial vehicle-based structure from motion technique for precise snow depth retrieval—implication for optimal ground control point deployment strategy. Remote Sensing, 2023; 15(9). https://doi.org/10.3390/rs15092297
24. Seo, D.-M., Choi, J., Lee, S. Optimization of Number of GCPs and Placement Strategy for UAV-Based Orthophoto Production. Applied Sciences, 2024; 14(8), 3163. https://doi.org/10.3390/app14083163
25. Szypuła, B. Accuracy of UAV-based DEMs without ground control points. GeoInformatica, 2024; 28(1). https://doi.org/10.1007/s10707-023-00498-1
26. Tkáč, M., Mésároš, P. Utilizing drone technology in the civil engineering. Selected Scientific Papers - Journal of Civil Engineering, 2019; 14(1). https://doi.org/10.1515/sspjce-2019-0003
27. Türk, T., Tunalioglu, N., Erdogan, B., Ocalan, T., Gurturk, M. Accuracy assessment of UAV-post-processing kinematic (PPK) and UAV-traditional (with ground control points) georeferencing methods. Environmental Monitoring and Assessment, 2022; 194(7). https://doi.org/10.1007/s10661-022-10170-0
28. Villanueva, J. R. E., Martínez, L. I., Montiel, J. I. P. DEM generation from fixed-wing UAV imaging and LiDAR-derived ground control points for flood estimations. Sensors (Switzerland), 2019; 19(14). https://doi.org/10.3390/s19143205
29. Yang, J., Li, X., Luo, L., Zhao, L., Wei, J., Ma, T. New supplementary photography methods after the anomalous of ground control points in UAV structure-from-motion photogrammetry. Drones, 2022; 6(5). https://doi.org/10.3390/drones6050105
30. Yu, J. J., Kim, D. W., Lee, E. J., Son, S. W. Determining the optimal number of ground control points for varying study sites through accuracy evaluation of unmanned aerial system-based 3d point clouds and digital surface models. Drones, 2020; 4(3). https://doi.org/10.3390/drones4030049
31. Zhao, H., Li, J., Wang, B., et al. Impacts of GCP Distributions on UAV-PPK Photogrammetry Projects. Remote Sensing, 2024; 16(21), 3934. https://doi.org/10.3390/rs16213934
32. Zhang, K., Okazawa, H., Hayashi, K., Hayashi, T., Fiwa, L., Maskey, S. Optimization of ground control point distribution for unmanned aerial vehicle photogrammetry for inaccessible fields. Sustainability (Switzerland), 2022; 14(15). https://doi.org/10.3390/su14159505
33. Zietara, A. M. Creating Digital Elevation Model (DEM) based on ground points extracted from classified aerial images obtained from Unmanned Aerial Vehicle (UAV). Norwegian University of Science and Technology Faculty of Engineering. Department of Civil and Environmental Engineering, 2017. (June).